Scientific paper

Behaviour of Strain-Hardening Cement-Based Composites Under High Strain Rates

Viktor Mechtcherine[1], Flávio de Andrade Silva[1], Marko Butler[1], Deju Zhu[2], Barzin Mobasher[2], Shang-Lin Gao[3] and Edith Mäder[3]

Received 7 July 2010, accepted 13 October 2010

Abstract

In this research project the behaviour of strain-hardening cement-based composites (SHCC) subjected to low and high strain rates was studied. Uniaxial tension tests on dumbbell-shaped SHCC specimens were performed at rates ranging from $10^{-5}s^{-1}$ to $50s^{-1}$. For the tests performed at strain rates of $10^{-2}s^{-1}$ and below, SHCC yielded a moderate increase in tensile strength and simultaneous decrease in strain capacity with increasing strain rate. When tested for higher strain rates from 10 to $50s^{-1}$ a considerable increase in tensile strain and strain capacity was measured. Microscopic investigation of the fracture surfaces showed that almost no fibre failure and an average pullout length of 2.5mm were found in the high strain rate test. This observation is in contrast to that of rapid quasi-static testing, where the average fibre pullout length of 300μm was much shorter. Furthermore, the fibres on the fracture surfaces produced in the high rate tests exhibited pronounced plastic deformations. Finally, quasi-static and high-speed tension tests on individual fibres and single fibre pullout tests were performed. While the increase in the tensile strength of the fibre was only moderate in the range of strain rates investigated, a considerable increase in bond strength between fibre and matrix was determined.

1. Introduction

Strain-hardening cement-based composites (SHCC) reinforced by short PVA fibres constitute a relatively new class of building material, which exhibits pseudo-strain hardening behaviour with multiple cracking formation when tested under tension loads at quasi-static strain rates (Li *et al*. 2001; Mechtcherine and Schulze 2005). The high ductility and strain capacity of SHCC (also referred to as engineered cementitious composites (ECC) (Li *et al*. 2001)) are exceptional for cement-based materials. They give this material a marked potential for use in applications in which high non-elastic deformability is needed. Some examples of very promising applications are link-slabs for jointless bridge decks (Lepech and Li 2005), structural repairs (Li 2004), and connecting beams for high-rise buildings in earthquake areas (Rokugo 2005).

Due to the ductility of SHCC, it might be expected that such material perform well when subjected to dynamic loading. On the other hand, the material's behaviour under high strain rates might be very different from that under quasi-static loading. Thus, the validity of stress-strain relations obtained in the quasi-static tests could be limited to low rate loading only. The use of such data in the analysis and design of dynamically loaded structures can lead either to overly cautious, weighty designs or to premature structural failure. Examples of common dynamic loading in concrete structures are fast moving traffic ($\dot{\varepsilon}$ of 10^{-6} to $5{\cdot}10^{-4}s^{-1}$), gas explosions ($5{\cdot}10^{-5}$ to $5{\cdot}10^{-4}s^{-1}$), earthquakes ($5{\cdot}10^{-3}$ to $5{\cdot}10^{-1}s^{-1}$), pile driving (10^{-2} to $1s^{-1}$) and aircraft landing ($5{\cdot}10^{-2}$ to $2s^{-1}$) (Banthia *et al*. 2004). Blast loading, aircraft impact or impact by hard projectiles can produce strain rates much higher than the instances cited above. A proper understanding of the response of concrete-based materials to such loading is important to the correct design of structures against which industrial explosions, terrorist bombings, or military attacks may occur.

While there is still a lack of knowledge about the material behaviour of SHCC under strain rates above $1s^{-1}$, few works have been published on its tensile behaviour at rates of up to $0.2s^{-1}$. Maalej *et al*. (2005) tested hybrid-fibre SHCC containing a combination of high-modulus steel fibres and relatively low-modulus polyethylene fibres under tensile loading at strain rates ranging from $2{\cdot}10^{-6}$ to $0.2s^{-1}$. With increasing strain rate, the tensile strength increased almost by two times but no obvious changes in the strain capacity (strain at failure) were observed. According to Yang and Li (2005), similarly, with strain rate increasing from 10^{-5} to $10^{-1}s^{-1}$, the tensile strength of SHCC also increases by two times whereas the strain capacity decreased from 3% to 0.5%. Furthermore, Douglas and Billington (2005) reported a 53% decrease in the strain capacity and a 12% increase in tensile strength of a SHCC tested at a strain rate of $0.2s^{-1}$ when compared to the results of quasi-static tests ($2x10^{-5}s^{-1}$). To explain these phenomena, discussion centred on a strengthening of the bond at the interface

[1]Institute of Construction Materials, TU Dresden, Dresden, Germany.
E-mail: viktor.mechtcherine@tu-dresden.de
[2]Department of Civil and Environmental Engineering, Arizona State University, Tempe, USA.
[3]Leibniz-Institut für Polymerforschung Dresden, Germany.

with increasing strain rate, which resulted in premature fibre failure. This suggests that no complete fibre delaminating from the matrix and subsequently no fibre pullout occurred at high loading rates. Boshoff *et al*. (2009) found additionally that the probability of fibre failure increased with increased loading rate. Furthermore, they showed by means of fibre pullout tests that an increase in the pullout rate could change the failure mechanism from gradual pullout to predominant fibre rupture.

With regard to very high loading rates only an investigation by Maalej *et al*. (2005), who studied the impact resistance of SHCC to projectiles, can be found in the literature. According to these results SHCC showed clearly beneficial behaviour in comparison to ordinary or high-strength concrete: increased shatter resistance with a nearly complete lack of scabbing, spalling, or fragmentation and much better energy absorption through distributed micro-cracking. Characterisation of the mechanical properties of SHCC was not the subject of that study.

The objective of the current work is to obtain more detailed knowledge of mechanical behaviour of SHCC under conditions of high-speed loading. With that in mind, uniaxial tensile tests on dumbbell-shaped specimens were carried out at rates ranging from $10^{-5}s^{-1}$ to $50s^{-1}$. The microstructure of the fracture surfaces was investigated to identify specific failure mechanisms of SHCC under high and low loading rates. Furthermore, low and high-speed pullout tests on individual PVA fibres embedded in SHCC matrices were performed in order to reveal the strain rate effects on the interfacial behaviour between the PVA fibres and the cement-based matrix. This test series was accomplished by tensile tests on single PVA fibres.

2. The experiment

2.1 Materials

The SHCC composition used in the present investigation is based on previous work by Mechtcherine and Schulze (2005). A combination of Portland cement 42.5 R and fly ash was utilized as binder. The aggregate was uniformly graded quartz sand with particle sizes ranging from 0.06mm to 0.20mm. PVA fibres in a volume fraction of 2.2%, measuring 12mm in length and 0.04mm in diameter (Kuraray Co., Ltd., Kuralon K-II REC15) were used as reinforcement. A super plasticizer on a polycarboxilate-ether basis (SP) and a viscosity agent (VA) were added to the mix in order to adjust its rheological properties.

Table 1 gives the mix proportions of the material developed. In comparison to the reference mix presented in Mechtcherine and Schulze (2005), the proportion of cement and fly ash was altered. Furthermore, a superabsorbent polymer (SAP) was used as a multi-tasking agent: (1) to reduce autogenous shrinkage, (2) to improve the frost resistance, and (3) above all, to introduce micro-defects, which are favourable with regard to inducing the formation of multiple cracks (see also Brüdern and Mechtcherine 2010).

Table 1 Mix proportions of SHCC under investigation.

Material	(kg/m^3)
Cement 42.5 R-HS (Heidelberger Cement)	505.00
Fly Ash	613.54
Quartz sand (0.06-0.20 mm)	534.22
Viscosity Agent	3.20
Superplasticizer (Glenium ACE 30)	16.58
Water	324.01
SAP	2.02
PVA – 12 mm (2.2 %)	29.30

The matrix was produced using a bench-mounted mixer of 20 litres capacity. The fines and sand were homogenized by dry mixing for 30s. Water mixed with one half of the super plasticizer was poured into the dry mix during 30s and mixed for an additional 60s. PVA fibres were added over a period of 30s and mixed for an additional 180s. The second half of the super plasticizer was added at this stage for 30s and mixed for another 180s. The mix was cast horizontally in steel moulds. The moulds were stored for 2 days in a room with controlled temperature (T = 25°C) and humidity (RH = 65%). After demoulding the specimens were sealed in plastic foil and stored at room temperature until testing.

2.2 Tensile testing of SHCC at different strain rates

Low-speed tensile test on SHCC

Figure 1 shows the specimen geometry used in both the low and high strain tensile tests on SHCC. The dumbbell specimens had a nominal cross-section of 40mm by 24mm at the narrow portion and a cross-section of 40mm by 40mm at the ends. The gauge length was 100mm.

The low-speed tension tests were performed on these specimens in an Instron servo-hydraulic universal testing machine. The tests were controlled by the actuator displacement at rates ranging from 0.001mm/s to 1mm/s, which, considering the applied gauge length of 100mm, corresponded to strain rates ranging from 10^{-5} to $10^{-2}s^{-1}$. The tops and bottoms of the dumbbell specimens were glued using a fast setting HBM glue to steel rings which were connected to the hydraulic grips of the testing machine, so the setup used had so-called fixed-fixed boundary conditions. The deformations could be continuously measured by means of two LVDT's fixed to the specimen as shown in **Fig. 1**. Six specimens were tested for each strain rate.

High-speed tensile test of composites

The high-speed tensile tests were performed in a high-rate MTS testing machine. The same specimen geometry as in quasi-static testing was used. The setup of the dynamic tensile testing is presented in **Fig. 2**. Once the

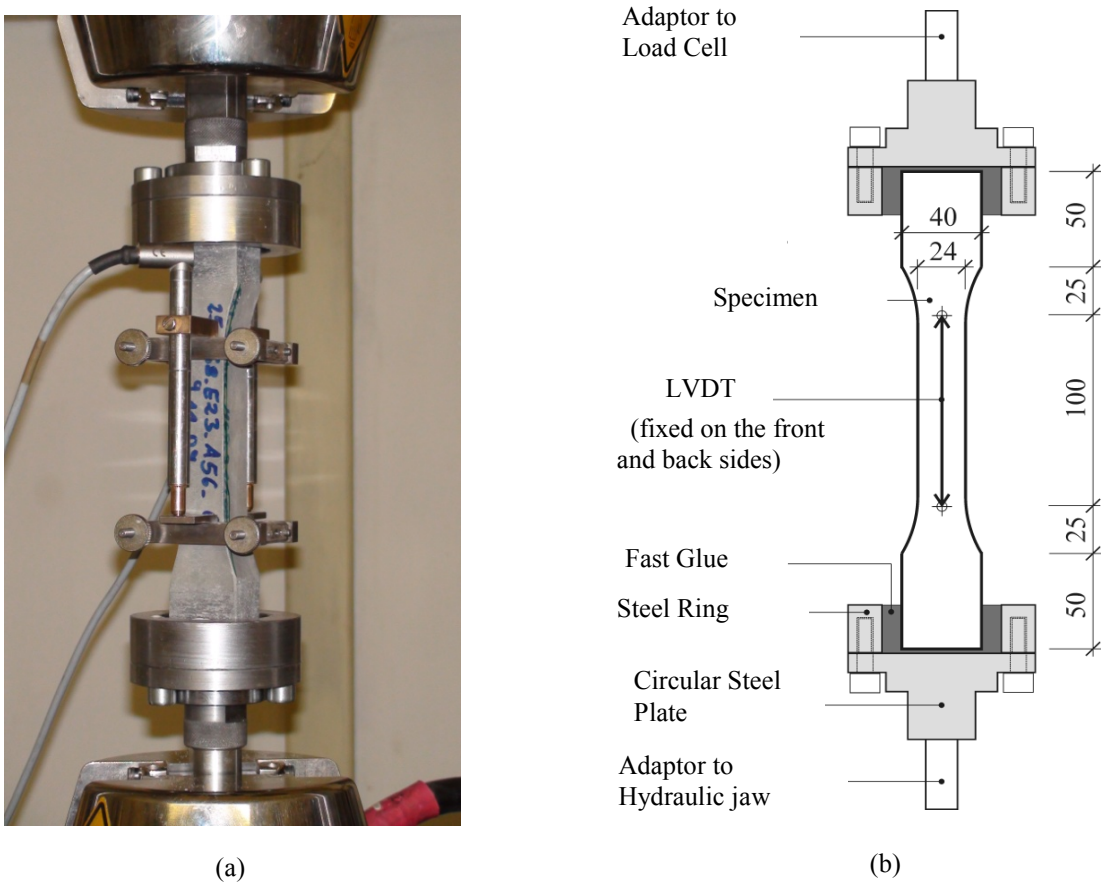

Fig. 1 Test setup for low-speed tensile testing: (a) picture of a dumbbell specimen, grips and instrumentation and (b) sketch showing the specimen geometry and details of grips (dimensions are given in mm).

test starts, the actuator accelerates to reach the specified speed and then maintains that rate. During this range of motion, the slack adaptor engages and transfers the force to the specimen. The slack adaptor consists of a sliding bar with a conical end that travels within a hollow tube. It travels freely with the actuator at the specified velocity before making contact with the cone-shaped surface of the sliding bar. This eliminates the effect of the inertia on the lower grip and actuator during acceleration. However, the sudden contact with the upper portion of the setup generates high amplitude stress waves, causing oscillations at the system's natural frequency, i.e. system ringing (Xiao 2008). To reduce the effect of inertia, lightweight grips made of stainless steel were used as sketched in **Fig. 2**. The tension tests were performed at strain rates of 10, 25 and 50s^{-1}. Six dumbbell-shaped specimens were tested for each strain rate.

The load was measured by a Kistler 9041A piezoelectric force link (load washer) with a capacity of 90kN, rigidity of 7.5kN/µm, and a frequency response of 33kHz. The load signal was amplified by a Kistler 5010B dual mode charge amplifier. A high-speed digitizer was used to record the force from the piezoelectric force link, and the response of the LVDT actuator, which measured the deformation of the specimen. A data acquisition system operated at a maximum rate of 5MHz. The signals from load washer and LVDT actuator were recorded at a sampling rate of 250kHz. High frequency noise was filtered using a low-pass filter with a cutoff frequency of 3Hz.

Material parameters derived from the experimental data included tensile strength (peak stress), strain capacity (strain on reaching tensile strength) and work to fracture. Work to fracture was calculated using the total area under the load-displacement curve. Average value and standard deviation are given for each strain rate. Furthermore, tensile stress-strain curves of the specimens tested under static and dynamic conditions are compared.

A representative sample of the recorded responses generated by the servo-hydraulic, high-rate testing setup is given in **Fig. 3** for a dumbbell specimen tested at a strain rate of 10s^{-1}. Here are presented the recorded force, displacement of stroke, and its corresponding velocity plotted over the entire time of the test. The test duration was less than 10 milliseconds with a nearly constant actuator velocity of 1000mm/s as shown by the

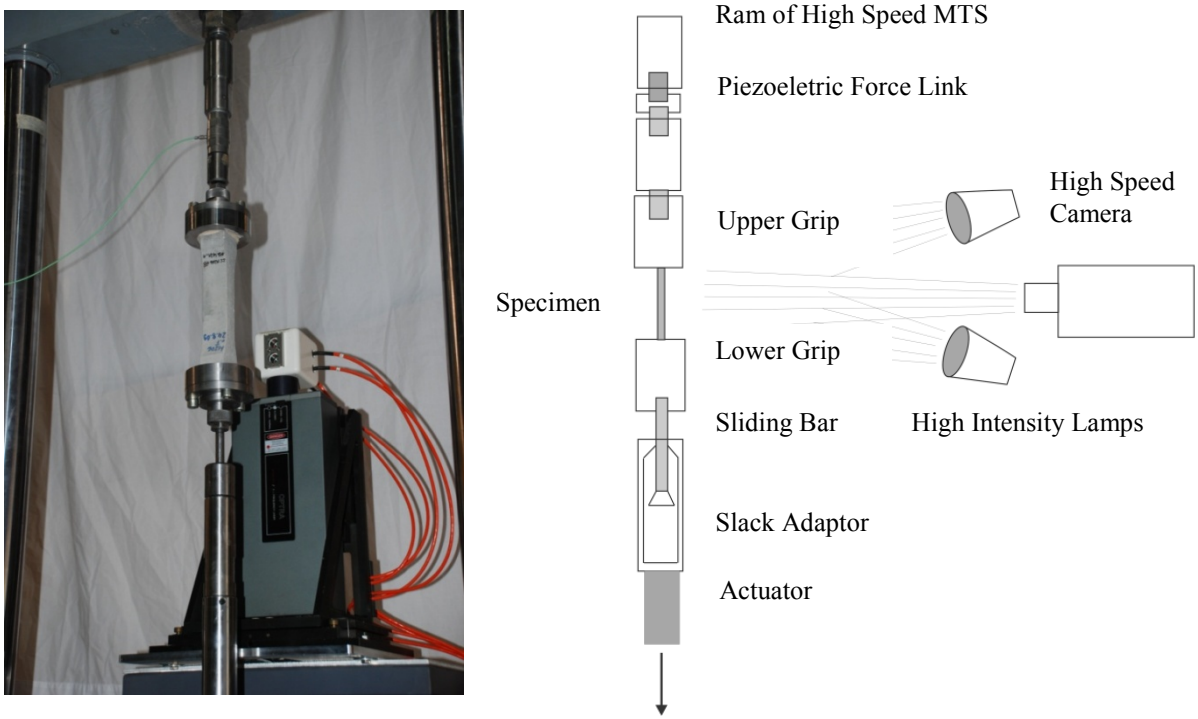

Fig. 2 Test setup for high-speed tensile testing: (a) picture of a dumbbell specimen, grips and high-speed camera, (b) schematic presentation.

linear course of the displacement-time relation (cf. **Fig. 3**). For further details of the high-speed tensile test methodology refer to Silva *et al*. (2010).

2.3 Single fibre tension and pullout tests at different strain rates

Tensile test on single PVA fibre

Experiments on single PVA fibres were conducted with a FAVIGRAPH Semiautomatic Equipment (Textechno, Germany) at velocities of 0.1, 2 and 180 mm/min, respectively. Associated with these velocities, the specimens with the gauge length of 2mm have strain rates of $8.3 \cdot 10^{-4}$, $1.7 \cdot 10^{-2}$ and $1.5 s^{-1}$, respectively. Approximately 50 single fibres for each strain rate were tested in order to determine the fibres' strength and strain capacity.

Fibre pullout test

A specialised single fibre pullout sample preparation and testing apparatus was used to conduct quasi-static investigations, the development of which is described in detail elsewhere (Mäder *et al*. 1994). The fibres were end-embedded 1mm deep into a cement matrix at 23°C ambient temperature and at a relative humidity of 50% and after 24h transferred to a desiccator and stored for 28 days at a relative humidity of about 90%. Based on the displacement rate of 0.01µm/s and the embedded fibre length of 1mm, the average strain rate of the embedded fibre in the pullout tests was approximately $10^{-5} s^{-1}$. For the production of specimens whose constant quality would reliably represent the fibre/matrix bond properties in SHCC, a locally made apparatus was used with PC-controlled temperature, time, and embedded

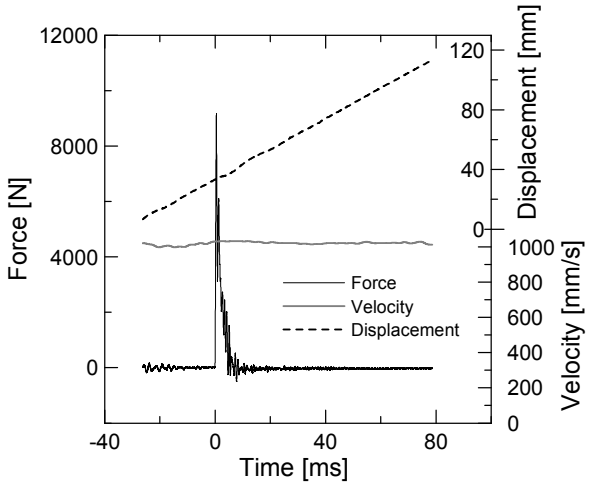

Fig. 3 Force history, displacement history of actuator, and its corresponding velocity history curves generated by the servo-hydraulic high-rate testing setup for a SHCC sample tested at a strain rate of $10 s^{-1}$.

length (Mäder *et al*. 2007). The original force-displacement curves and force-time curves were compared with those recorded during loading at high strain rates. The average force-displacement curve was obtained from the force-displacement curves of at least 10 tested samples.

For the high-speed pullout test a device was used which had been locally built for cyclic pullout tests in order to study the dynamic behaviour in a regime of frequency 5-350Hz. **Figure 4** shows a schematic view of this device described in detail elsewhere (Brodowsky *et al*. 2009). The setup consists of a single fibre with one end embedded into a 2mm-thick matrix droplet positioned on an aluminium sample holder. Essential to such a measurement is the high stiffness and play-free displacement of the equipment, whose main element is a piezo-electric force sensor. To perform high-speed tensile loading, a new software program and controller were developed for the equipment with a maximum displacement of 80µm and a maximum force of 50N. The software program made possible very rapid force generation and displacement registration at a transfer time of 0.5µs, which corresponds to a data collection frequency of 2MHz. The displacement rate was 10^{4}µm/s which corresponds to a nominal strain rate of $10^{1}s^{-1}$ if the displacement rate is related to the embedded length of 1mm. At the low and high speed regimes 10 pullout samples were tested.

2.4 Microscopy and topographic morphology

The fracture surfaces of SHCC prisms as well as the condition of the individual fibres after testing were studied using an optical microscope (OM) and a scanning electron microscope (ESEM). Additionally, topographic morphologies of the fibres' surfaces after pullout testing at different rates were investigated by means of an atomic force microscope (AFM) (Digital Instruments D3100, USA).

3. Results and discussion

3.1 Strain rate effect on the tensile behaviour of SHCC

Figure 5a shows one representative stress-strain curve obtained for each strain rate below $10^{-2}s^{-1}$. The results of the evaluation of all curves are given in **Table 2**. From these data it can be seen that the tensile strength increases from 4.5MPa to 5.5MPa while the elastic modulus rises from 19.7GPa to 23.9GPa as the strain rate increases from 10^{-5} to $10^{-2}s^{-1}$, see **Table 2** and **Fig. 6**. At the same time the average strain capacity decreases from 1.5% to 0.8% and the work to fracture also de-

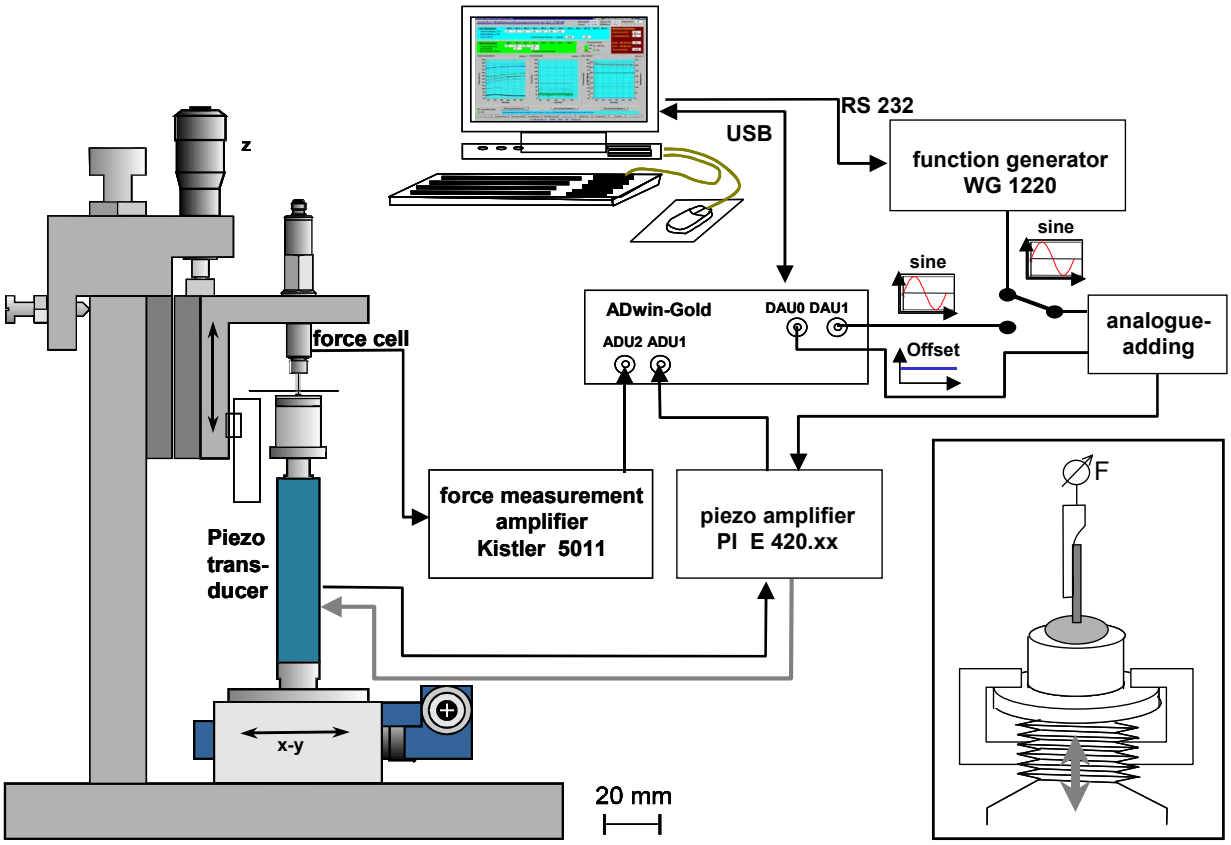

Fig. 4 Schematic view of the device for testing single fibre pullout behaviour; inset bottom right: detailed scheme of the specimen carrier within the test setup.

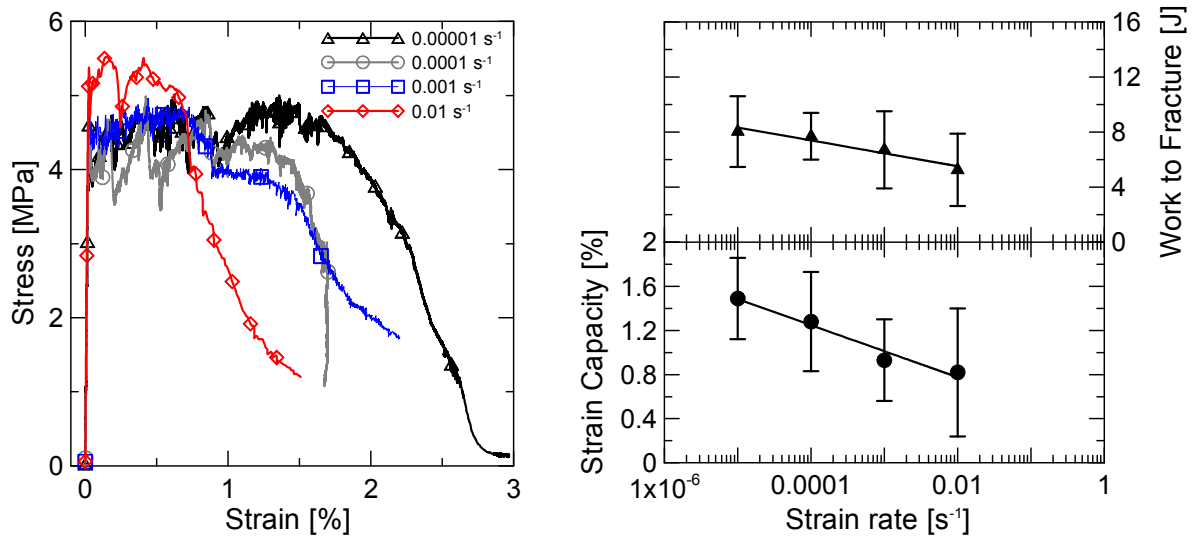

(a) (b)

Fig. 5 Effect of strain rate on the tensile behaviour of SHCC at low strain rates (≤ 0.01s^{-1}): (a) tensile stress-strain responses of SHCC, (b) effect of strain rate on the strain capacity and work to fracture of SHCC.

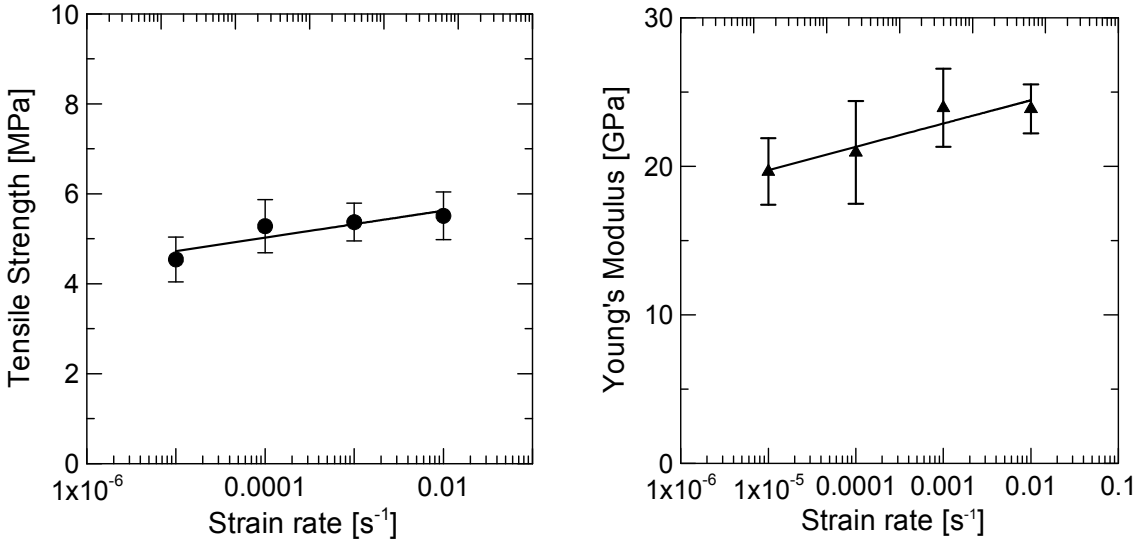

(a) (b)

Fig. 6 Effect of strain rate on (a) tensile strength and (a) elastic modulus of SHCC subjected to low strain rates (≤ 0.01s^{-1}).

creases from 8.0J to 5.3J (cf. **Table 2** and **Fig. 5b**). The strain capacity was defined as the strain at which the localization of failure occurs, i.e. the increase in deformation results from the opening of just one major crack, the stress level starts to decrease and all other cracks gradually close. While the behaviour of SHCC under quasi-static tensile loading at the very low rate of $\dot{\varepsilon}$ = 10^{-5}s^{-1} was characterised by a rather pronounced strain-hardening response accompanied by multiple cracking, the SHCC response on higher, but still quasi-static rates (up to 10^{-2}s^{-1}), revealed measurably less ductile behaviour and less multiple cracking. Similar rate dependence behaviour was also observed by Yang and Li (2005) and Douglas and Billington (2005). Within this range of strain rates the increase in strength and decrease in strain capacity is due to an increase in the bond strength between fibre and matrix according to reported pullout experiments performed at different strain rates (Boshoff

Table 2 Summary of low and high-speed tension test results; average results (standard deviations are given in parentheses).

Strain rate [s^{-1}]	Test velocity [m/s]	Tensile Strength [MPa]	Strain Capacity [%]	Young's Modulus [GPa]	Work to Fracture [J]
0.00001	0.000001	4.54 (0.50)	1.49 (0.37)	19.66 (2.25)	8.04 (2.56)
0.0001	0.00001	5.28 (0.59)	1.28 (0.45)	20.94 (3.46)	7.69 (1.70)
0.001	0.0001	5.37 (0.42)	0.93 (0.37)	23.94 (2.63)	6.71 (2.79)
0.01	0.0001	5.51 (0.53)	0.82 (0.58)	23.88 (1.65)	5.25 (2.62)
10	1.0	7.81 (1.35)	0.68 (0.28)	- -	9.86 (2.35)
25	2.5	12.08 (2.04)	0.86 (0.11)	- -	10.51 (2.07)
50	5.0	11.93 (0.86)	1.79 (0.32)	- -	20.03 (2.29)

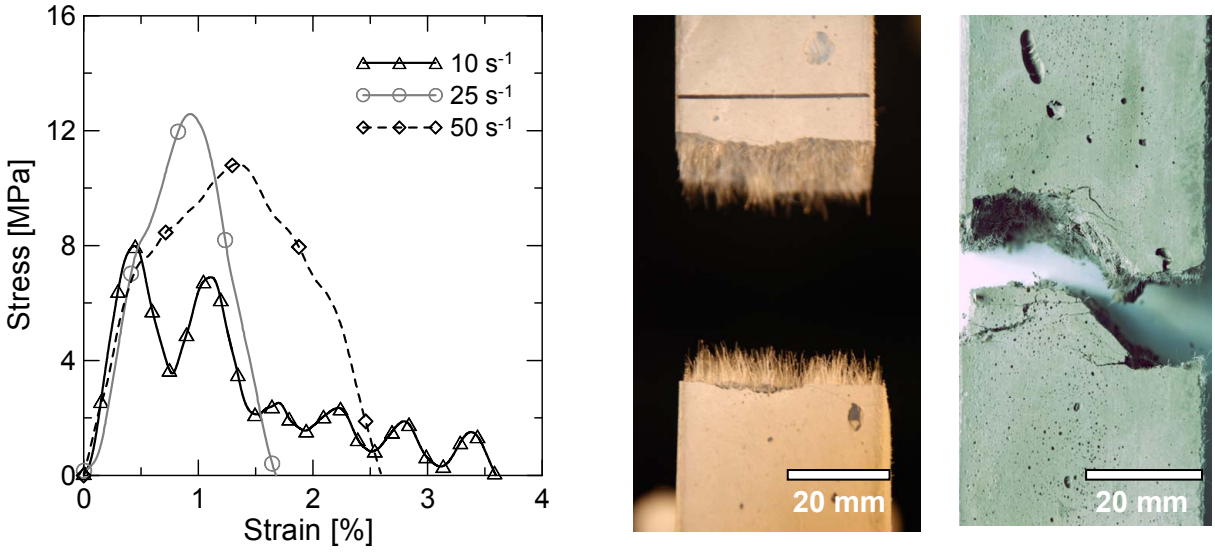

(a) (b) (c)

Fig. 7 Effect of strain rate on the tensile behaviour of SHCC at high strain rates (≥ $10s^{-1}$): (a) tensile stress-strain response of SHCC, (b) pronounced fibre pullout failure on the fracture surface of a sample tested at a rate of $25s^{-1}$, and (c) fracture surface of a sample tested at a rate of $0.001s^{-1}$.

et al. 2009). As a result of the higher bond strength, fibre failure becomes more frequent, with a decrease in the frequency of fibre pullout, leading to a more brittle failure of the composite as a whole.

Figure 7a shows typical stress-strain curves obtained for the high strain rates (≥$10s^{-1}$) on SHCC specimens. The shapes of the curves differ significantly to those obtained for lower strain rates. The strain-hardening effect seems to be very pronounced for SHCC tested on 25 and $50s^{-1}$. At the strain rate of $10s^{-1}$ some oscillation of the system at its natural frequency could be observed, which made the evaluation of the results complicated.

The material parameters derived from the measured data are given in **Table 2**. An increase in both tensile strength and strain capacity (**Fig. 7a** and **8**) was measured as the strain rate increased from 10 to $50s^{-1}$ (see **Table 2**). The explanation for the tensile strength's being nearly the same at the strain rates of 25 and $50s^{-1}$ has still to be found; however, the overall tendency is clear. The total work to fracture increased with increasing strain rate as well (**Fig. 8**), from 9.9J ($\dot{\varepsilon}$ = 10 s^{-1}) to 20.0J ($\dot{\varepsilon} = 50s^{-1}$).

The effect of strain rate on strength and other material parameters is illustratively represented by a parameter called the Dynamic Increase Factor (DIF). It is defined as the ratio of the dynamic-to-static material parameters. In this study the values measured at the lowest strain rate of $10^{-5}s^{-1}$ were considered to be the reference (static loading rate). **Figure 9** shows DIF values for the tensile strength DIF of SHCC under investigation. DIF ranged

from approximately 1.2 for the moderate strain rate $\dot{\varepsilon}$ of $10^{-4}s^{-1}$ to 2.5 for high-speed loading rate of $50s^{-1}$. The diagram indicates that the increase in DIF is moderate and nearly linear (in the given coordinate system with a logarithmic scale for the strain rate) at strain rates up to approximately $1s^{-1}$ to $10s^{-1}$ followed by a much steeper increase in DIF at higher strain rates. This general tendency is well known for other cement-based materials such as ordinary concrete, high-performance concrete or ultra-high-performance concrete with or without fibre-reinforcement (Millon *et al*. 2010). Depending on the particular material and the experimental setup, the transition from the moderate to the pronounced increase of DIF for tensile strength values was observed in the range from 1 to $10s^{-1}$. In Millon *et al*. (2010) SHCC was tested using the Hopkinson bar technique in the spallation configuration at strain rates of 140 to $180s^{-1}$. A comparison of those results with the results of the quasi-static testing yields a tensile strength DIF of 6.7, which shows that the pronounced increase of strength continues also for strain rates higher than those used in the present study.

Figure 10 depicts the strain rate effect on strain capacity and work to fracture of SHCC for all testing rates used in this investigation, the corresponding numeral data is given in **Table 2**. The results indicate that as a function of strain rate level there are two distinct behaviour patterns that were classified as modes A and B. In mode A (strain rates below $1s^{-1}$) as the strain rate increases the fibre-matrix bond strength also rises, leading to an increase in the strength of SHCC but also to a decrease in its strain capacity. In this range of strain rates, the cracking density was observed to be decreasing as a function of increasing rate, and the fracture mode is dominated by fibre failure rather than by fibre pullout. Mode B (strain rates above $1s^{-1}$) is characterised by fibre-matrix pullout failure, which leads to an increase in strain capacity and work to fracture. However, no multiple cracking patterns were observed under these high strain rates.

Macroscopic observations of the samples tested with strain rates of $10s^{-1}$ and higher showed a much more pronounced pullout length than with samples tested at strain rates of $10^{-2}s^{-1}$ or lower (cf. **Figs. 7b** and **7c**). Microscopic investigation of the fracture surfaces using ESEM illustrated these particularities even more clearly. **Figures 11a** and **11b** compare the fracture surface of a sample tested at a strain rate of $10^{-3}s^{-1}$ and another tested at $25s^{-1}$. The fibre pullout length measures several millimetres in specimens tested at the higher rate whereas the corresponding lengths observed for the specimens tested at $10^{-3}s^{-1}$ were considerably lower, less than 0.5mm in most cases. This can easily be traced back to the occurrence of pronounced fibre failure during the fast quasi-static tests. **Figure 11c** provides a closer look at a fibre which failed during the loading of a SHCC specimen, where a marked narrowing of the failed fibre indicates considerable local plastic deformations. The

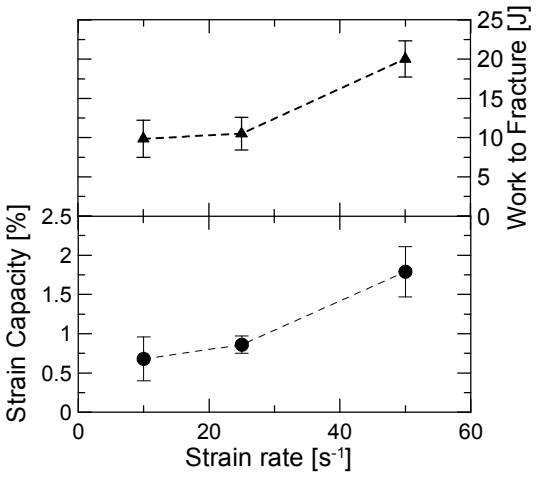

Fig. 8 Effect of strain rate on strain capacity and work to fracture of SHCC for rates ranging from 10 to $50s^{-1}$.

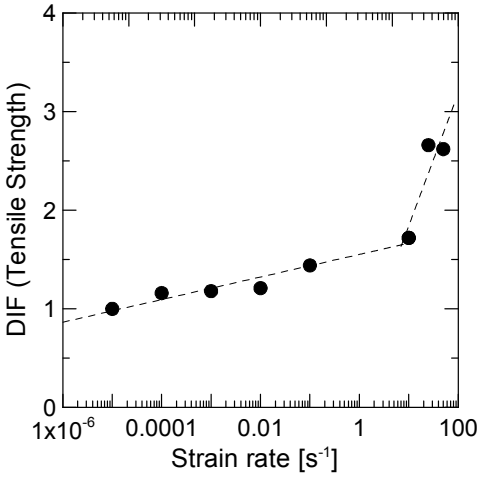

Fig. 9 DIF for tensile strength of SHCC.

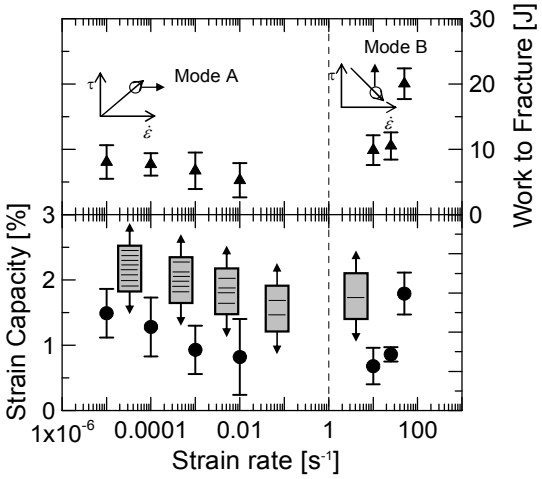

Fig. 10 Strain rate effect on strain capacity and work to fracture of SHCC tested under tensile load at rates ranging from $10^{-5}s^{-1}$ to $50s^{-1}$.

distance from the fracture surface of the matrix to the failure end of the fibre is approximately 0.3mm. At this stage it cannot be said with assurance exactly to what degree the delaminating of the PVA fibre from the matrix took place; what part of the protruding fibre length should be attributed to plastic deformations of fibre; and to which extent "true" fibre pullout occurred.

For strain rates higher than $10s^{-1}$ fibre pullout with an average free length of approximately 2.5mm was the main failure mechanism although a few ruptured fibres were observed as well. **Figure 11d** shows the capacity of PVA fibre to bridge cracks of approximately 200μm; this image was made of a specimen tested at a strain rate of $25s^{-1}$. Even though the SHCC does not show visible multiple cracking at strain rates of $10s^{-1}$ and above, its increased pullout length and crack-bridging capacity provide high strain capacity and work to fracture in this rage of strain rates. Plastic deformations of PVA fibre seem to play a much more important role in the case of high-speed loading. **Figures 12a** and **12b** show two micrographs of fibres pulled out from SHCC matrix at rates of $10^{-3}s^{-1}$ and $25s^{-1}$, respectively. A smoother surface in the fibre pulled out at the lower strain rate is to be seen. At strain rates higher than $10s^{-1}$ the fibres undergo during pullout a severe deformation process, which contributes considerably to the energy absorption capacity of the composite.

3.2 Strain rate effect on the mechanical behaviour and pullout behaviour of PVA fibre

Table 3 summarizes the results of the single fibre tension tests. Within the strain rate region tested a slight increase of the tensile strength with increasing strain rate was determined. The ultimate strain at failure remained unaffected by the change in loading rate.

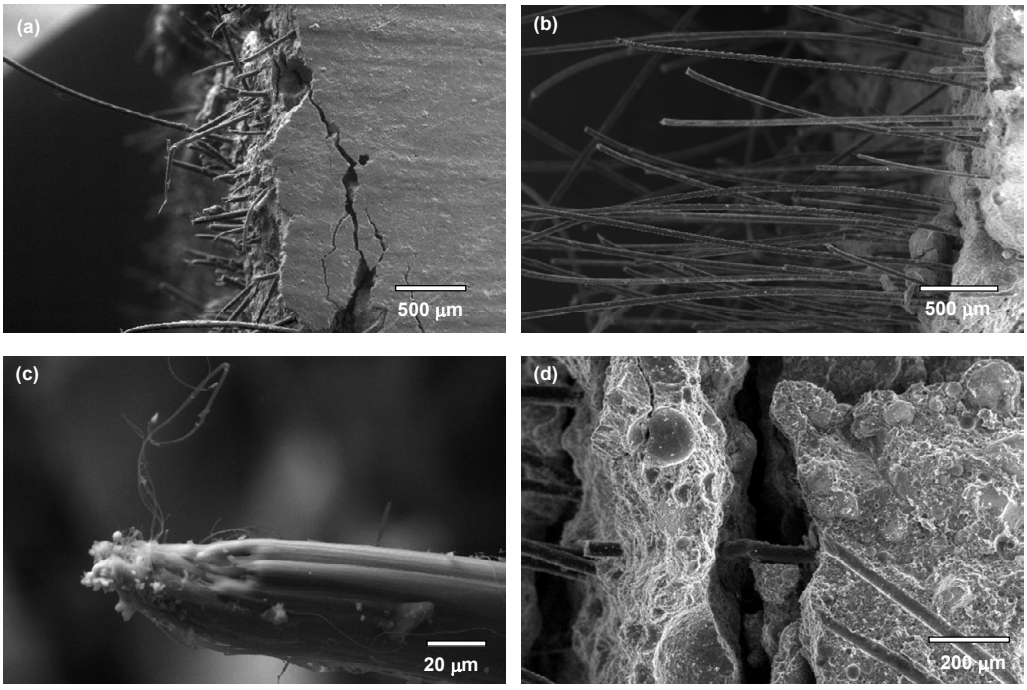

Fig. 11 Failure mechanisms of SHCC at low and high strain rates: (a) fracture surface of a specimen tested at $10^{-3}s^{-1}$ (b) fracture surface of a sample tested at $25s^{-1}$ (c) typical fibre fracture from (a), and (d) crack bridged by PVA fibre after being tested at $25s^{-1}$.

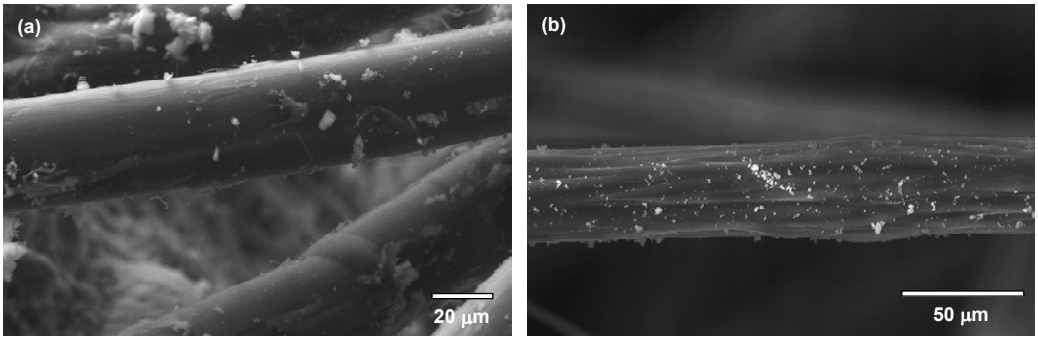

Fig. 12 Fibre surface after being pulled-out from SHCC matrix at (a) a strain rate of $10^{-3}s^{-1}$ and (b) $25s^{-1}$.

Table 3 Mechanical properties of PVA fibres in dependence on the strain rate (standard deviations are given in parentheses).

Gauge length [mm]	Speed [mm/min]	Strain rate [s^{-1}]	Diameter [μm]	Tensile strength [MPa]	Strain at failure [%]
2	0.1	0.00083	38.0 (2.8)	1456 (113)	27.4 (3.9)
2	2	0.017	37.3 (4.4)	1544 (162)	27.4 (4.0)
2	180	1.5	37.3 (3.7)	1674 (164)	27.5 (2.8)

The single fibre pullout tests performed with PVA fibre embedded in cement matrix were performed at quasi-static ($10^{-5}s^{-1}$) and high loading rates. Since the tensile loading is introduced into the system via the fibre, it is assumed that at low strain rates the loading rate of the entire embedded length is constant, whereas at high rates, the initial part of the embedded fibre is loaded at the applied strain rate. However, the deeper embedded part of the fibre might be loaded with a much lower strain rate. This assumption is still to be proven, but it seems quite plausible, since the parts of the fibre embedded into the matrix must first debond from the matrix before they can be substantially deformed (at high strain rate). The debonding process requires some time, which means some decrease in the local strain rate. **Figure 13** shows two typical force-time curves of high-speed loading and quasi-static pullout tests in comparison. A significant increase (by factor 2 approximately) of the maximum force at interfacial debonding occurs when the strain rate is increased. Another observation is that the maximum force is reached in the quasi-static pullout tests at a greater displacement than in the high-speed tests (**Fig. 14**). It should be mentioned that the peak load in the case of high-speed loading was reached at about 3ms during the test and that the piezotransducer stopped at 40μm displacement, i.e. not entire force-displacement relation could be recorded. Furthermore, it is unclear what the actual pullout rate was. Near the cement paste surface it might be the highest decreasing rapidly with increasing distance from the surface. Further investigations are needed to clarify this issue.

Some additional insight could be obtained from the observation of fibre surface after the pullout experiments. The representative SEM and AFM microphotographs (**Fig. 15**) show some differences for PVA fibres after pullout tests at low quasi-static and high-strain loading. The original fibre surface with texture grooves can be clearly seen for the former case while the fibre surface is coated partly with the matrix material for the latter case. The increasing loading rate seems to lead to an enhanced interface bonding strength which might arise from the change from adhesive failure involving fibre-matrix interface debonding to partly cohesive failure within the interphase, which in turn might exert major influence on the tensile properties of SHCC.

The results of fibre tension and pullout experiments agree well with the results of uniaxial tension tests on SHCC performed at quasi-static rate (e.g. $10^{-5}s^{-1}$) and elevated strain rates (10^{-2} s^{-1}). Since the increase in strain rate lead only to a moderate increase in fibre strength but at the same time to a considerable increase of the pullout resistance, fibre failure dominates the failure at elevated rate rather than fibre pullout. It is still to be investigated, however, why the failure mode

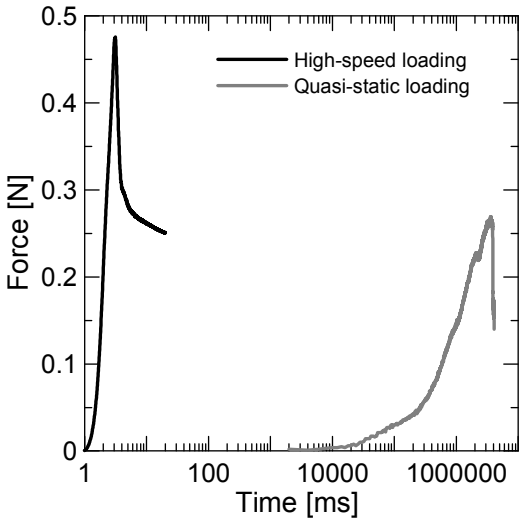

Fig. 13 Force-time curves of high-speed loading and quasi-static loading of single PVA fibre / cement composites at an embedding length of 1mm.

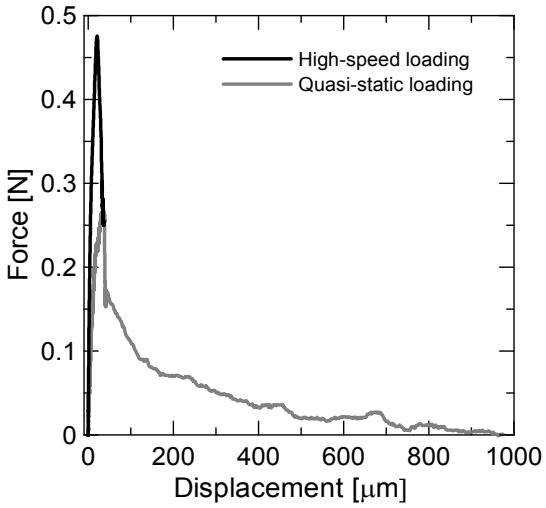

Fig. 14 Typical force-displacement curves of a PVA-fibre pulled out of a cement matrix at a strain rate of $10^{-5}s^{-1}$ (drive velocity 0.01μm/s) in comparison with high-speed loading at a strain rate of $10^{1}s^{-1}$ (drive velocity 10^{4}μm/s).

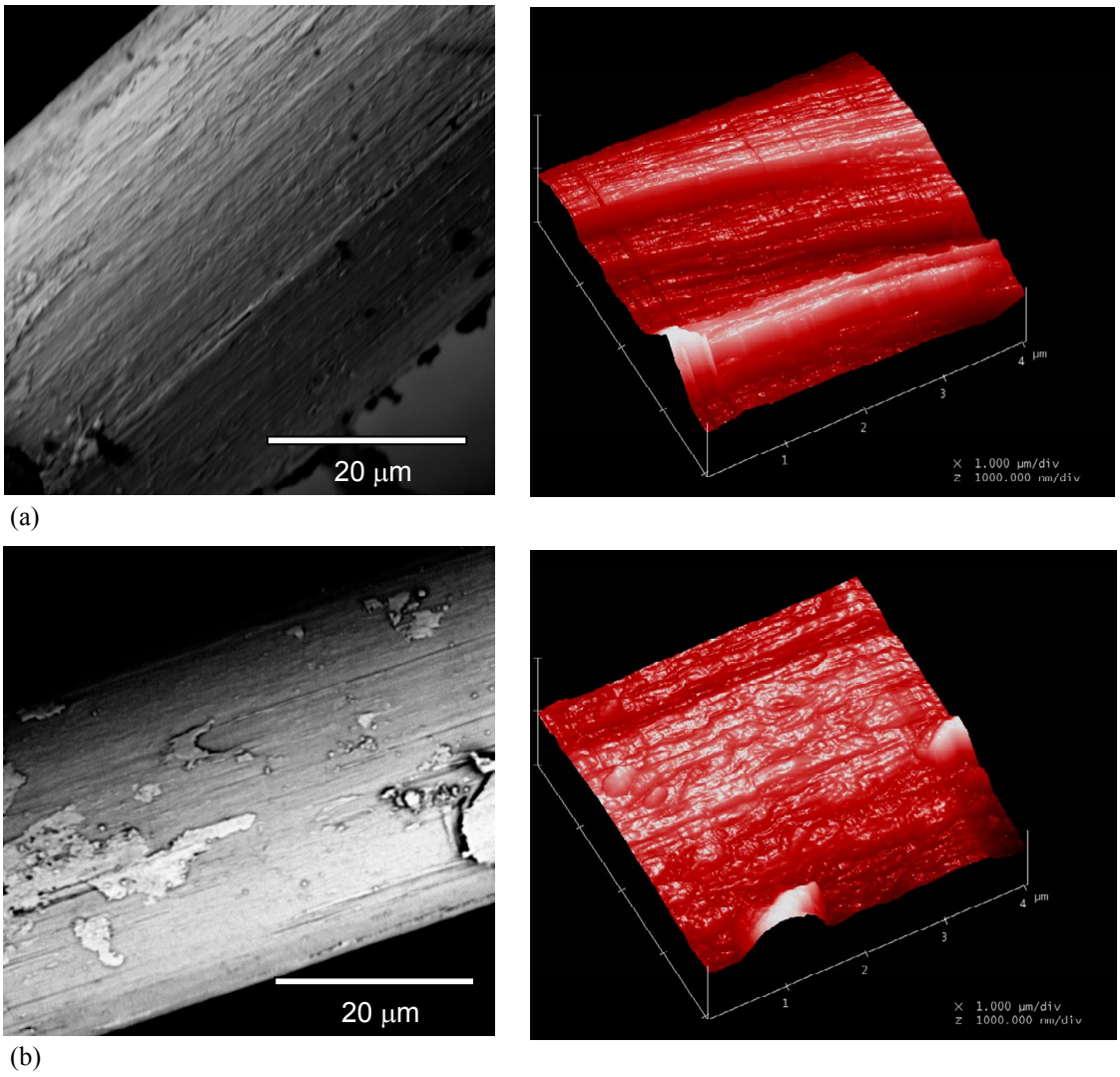

(a)

(b)

Fig. 15 SEM (left) and AFM (right) topographic images of fracture surfaces of PVA-fibres (a) pulled out of a cement matrix at a strain rate of 10^{-5} s^{-1} (drive velocity 0.01μm/s) compared with (b) high-speed loading at a strain rate of $10^{1}s^{-1}$ (drive velocity 10^{4}μm/s).

changes again to fibre pullout when the loading rate further increases (as it was observed at the tension tests on SHCC at very high strain rates). Furthermore, it should be clarified what displacement rates applied in the fibre pullout tests correspond to real fibre pullout rates in a crack plane at a given strain rate applied to an SHCC specimen.

4. Conclusions

The following conclusions can be drawn from the present work on the behaviour of SHCC under high tensile strain rate loading:

(1) For tension tests performed at strain rates up to $10^{-2}s^{-1}$, SHCC with increasing strain rate exhibited an increase in tensile strength and a decrease in strain capacity. The number of cracks at the composite failure decreased as the strain rate increased, and a predominance of fibre failure was observed at higher strain rates. Characteristically the failed fibres protruded less than 0.5 mm out of the matrix. This behaviour has been explained with reference to the increase in the strength of the fibre-matrix bond with increasing strain rate as it was observed in the accompanying pullout tests on single fibres.

(2) When loaded at high strain rates ranging from 10 to $50s^{-1}$ in this study, SHCC showed an increase in both tensile strength and strain capacity with increasing loading rate. No pronounced multiple cracking was observed. However, the failure of the composite was accompanied by the pullout of most of the fibres crossing the macro-crack. The average pullout length was approximately 2.5mm. Furthermore, numerous fibres showed a high degree of plastic deformation, which was related to the high-speed pullout process. The authors be-

lieve that the increase in fibre pullout length and the plastic deformation of the fibres are the main mechanisms leading to the observed increase in the strain capacity of SHCC at the strain rates over $10s^{-1}$.

References

Banthia, N., Bindiganavile, V. and Mindess, S., (2004). "Impact and blast protection with fiber reinforced concrete." In: *6th Rilem Symposium on Fiber Reinforced Concretes - BEFIB*, Varenna, Italy, 2004, 31-44.

Boshoff, W. P., Mechtcherine, V. and van Zijl, G. P. A. G., (2009). "Characterising the time-dependant behaviour on the single fibre level of SHCC: Part 2: The rate effects on fibre pull-out tests." *Cement and Concrete Research,* 39(9), 787-797.

Brodowsky, H., Jenschke, W. and Mäder, E., (2009). "Characterization of interphase properties by frequency dependent cyclic loading of single fibre model composites." *Journal of Adhesion Science and Technology,* 24, 237-253.

Brüdern, A.-E. and Mechtcherine, V., (2010). "Multifunctional use of SAP in Strain-hardening Cement-based Composites." In: *International RILEM Conference on Use of Superabsorbent Polymers and Other New Additives in Concrete*, Lyngby, 11-22.

Douglas, K. S. and Billington, S. L., (2005). "Rate dependencies in high-performance fibre reinforced cement-based composites for seismic application." In: *International RILEM Workshop on High Performance Fiber Reinforced Cementitious Composites (HPFRCC) in Structural Applications, Honolulu, Hawaii,* RILEM S.A.R.L.,17-25.

Lepech, M. and Li, V. C., (2005). "Design and Field Demonstration of ECC Link Slabs for Jointless Bridge Decks." In: *3rd International Conference on Construction Materials: Performance, Innovations and Structural Implications (ConMat'05)*, Vancouver, British Columbia, CD-documents.

Li, V. C., Wang, S. and Wu, C., (2001). "Tensile strain hardening behavior of polyvinyl alcohol engineered cementitious composites (PVA-ECC)." *ACI Materials Journal*, 98, 483-492.

Li, V. C., (2004). "High Performance Fiber Reinforced Cementitious Composites as Durable Material for Concrete Structure Repair." *International Journal for Restoration*, 10(2), 163-180.

Maalej, M., Quek, S. T. and Zhang, J., (2005). "Behaviour of hybrid-fibre engineered cemetitious composites subjected to dynamic tensile loading and projectile impact." *Journal of Materials in Civil Engineering,* 17(2), 143-152.

Mäder, E., Grundke, K., Jacobasch, H. J. and Wachinger, G., (1994). "Surface, interphase and composite property relations in fibre-reinforced polymers." *Composites*, 25(7), 739-744.

Mäder, E., Gao, S.-L., Plonka, R. and Wang, J., (2007). "Investigation on Adhesion, Interphases, and Failure Behaviour of CBT/ Glass Fiber Composites." *Composites Science and Technology,* 67, 3140-3150.

Mechtcherine, V. and Schulze, J., (2005). "Ultra-ductile concrete – material design concept and testing." *CPI Concrete Plant International*, (5), 88-98.

Millon, O., Mechtcherine, V., Thoma, K. and Butler, M., (2010). "Verhalten von hochduktilem Beton unter Impaktbelastung." *Beton- und Stahlbetonbau,* 105(7), 445-454.

Rokugo, H., (2005). "Applications of Strain Hardening Cementitious Composites with multiple cracks in Japan." In: Mechtcherine, V. (Ed.) *Ultra-ductile concrete with short fibre - Development, Testing, Applications*, ibidem Verlag, 121-133.

Silva, F. A., Zhu, D., Mobasher, B., Soranakom, C., Toledo Filho, R. D., (2010). "High speed tensile behavior of sisal fiber cement composites." *Materials Science and Engineering- A*, 527(3), 544-552.

Xiao, X., (2008). "Dynamic tensile testing of plastic materials." *Polymer Testing*, 27(2), 164-178.

Yang, E. and Li, V. C., (2005). "Rate dependence in engineered cementitious composites." In: *International RILEM Workshop on High Performance Fiber Reinforced Cementitious Composites (HPFRCC) in Structural Applications, Honolulu, Hawaii,* RILEM S.A.R.L., 83-92.